Journal of Water Sustainability, Volume 4, Issue 3, September 2014, 167-180

Monitoring of Membrane Scaling and Concentration Polarization in Spiral-Wound Reverse Osmosis Module Using Ultrasonic Time-Domain Reflectometry with Sound Intensity Calculation

Xianhui Li, Genghong An, Jiebin Lin, Jianxin Li*

State Key Laboratory of Hollow Fiber Membrane Materials and Processes, School of Materials Science and Engineering, Tianjin Polytechnic University, Tianjin 300387, China

ABSTRACT

Ultrasonic time-domain reflectometry (UTDR) with a sound intensity calculation was used to monitor membrane scaling and concentration polarization in a 4-inch spiral-wound reverse osmosis module. Three focused transducers with the frequency of 2.25 MHz were located equidistantly on the module along the feed flow direction. The scaling experiments were carried out with 1.0 g/L and 2.0 g/L calcium sulfate for 90 h fouling. Results show that the membrane surface suffered from more severe fouling at the high solution concentration of 2.0 g/L $CaSO_4$. And the fouling degree gradually increased along the flow direction of RO module. Furthermore, the sound intensity obtained at the solution of 1.0 g/L $CaSO_4$ gradually increased during the fouling process, whereas the sound intensity obtained at solution of 2.0 g/L $CaSO_4$ gradually decreased to minimum at first, then increased due to concentration polarization as well as the deposition and growth of fouling layer. Moreover, the initial induction time in the change of sound intensity is related with the degree of concentration polarization. It could be an indicator for the start of foulant deposition. The independent methods such as SEM and weight measurements were in good agreement with the ultrasonic observations.

Keywords: Reverse osmosis; membrane scaling; concentration polarization; ultrasonic time-domain reflectometry (UTDR); sound intensity

1. INTRODUCTION

Reverse osmosis (RO) is the most widely used in desalination technology globally, due to the high permeation flux, easy operation, and minimal chemical addition. Currently, over half of the 15,000 desalination plants worldwide are using RO processes, and the growth of RO desalination capacity is expected to continue. However, membrane fouling still remains as a major obstacle for a wider use of RO membrane, which leads to the deterioration of water permeability and increase of operation cost (Mulder, 1991). As one of the major components in the RO desalination, concentration polarization is the most persistent problem.

In order to investigate the characteristic of fouling behavior and concentration polarization phenomenon, a number of studies have been carried out recently. Chong et al. (2007) developed a sodium chloride tracer response technique to determine the effect of fouling on concentration polarization level in a RO system at a constant flux operating mode. It was found that the formation of fouling layer greatly exacerbated the concentration polarization level in RO separations with a more

*Corresponding to: jxli@tjpu.edu.cn

DOI: 10.11912/jws.2014.4.3.167-180

pronounced effect at high flux operation. Chong et al. (2008) further described a systematic study of biofouling in RO process using model bacteria *pseudomonas fluorescens* and employing a sodium chloride tracer response technique for fouling characterization. The results showed that the imposed flux determined the level of concentration polarization through the interplay between concentration polarization and nutrient concentrations at the membrane wall. Song et al. (2012) set up a total salt balance model to investigate the effect of shear flow in crossflow reverse osmosis channels on the concentration polarization. And the new model indicated that a stronger concentration polarization would develop in the membrane channel with shear flow when the same average crossflow velocity was maintained.

Although these above studies provide insight into the RO fouling mechanism, the actual mechanism of fouling deposition remains incompletely understood due to the lack of additional techniques to detect the foulant deposition processes. Therefore, the novel non-invasive, in-situ and quantitative assessment of characteristics of the fouling layer growth is essential to deeply understand the fouling mechanic, so as to facilitate the strategies for membrane fouling prevention and control.

For more than a decade the ultrasonic time domain reflectometry (UTDR) has successfully been used to study membrane processes, especially in the RO system. Mairal et al. (1999, 2000) first employed UTDR technique for the real-time characterization of calcium sulfate fouling and cleaning of flat-sheet RO membranes. The results showed a good correspondence between the change of ultrasonic signal amplitude and the development/removal of a scaling layer. Sanderson et al. (2002) further developed UTDR technique for improved visualization of calcium carbonate fouling in RO modules. Based upon the previous studies, Li et al. (2005) further investigated the deposition processes of calcium sulfate on RO membranes using UTDR technique and a simplified model. They showed that a fouling echo obtained in the time domain could indicate the actual state of a fouling layer on a membrane surface.

To further investigate the scaling process in the spiral-wound modules, Chai et al. (2007) employed UTDR associated with gravimetric and SEM analyses to study fouling in spiral wound membrane modules. It was found that changes of signal amplitude are more sensitive than those of the flux. Zhang et al. (2007) described the extension of UTDR for the measurement of scaling and cleaning in commercial spiral-wound RO modules. The results indicated that the overall flux decline is reasonably correlated with the changes in both the amplitude and the arrival time shift factors. In order to explore a more detailed and suitable analysis of the ultrasonic response signals, An et al. (2011) developed a signal analysis protocol of sound intensity calculation and modeling to in situ monitor the membrane fouling and cleaning in spiral-wound RO modules. According to this study, the systematic changes in the response signals and its total sound intensity were correlated to the deposition and removal of the scaling during the $CaSO_4$ fouling experiment. Overall, the previous studies have demonstrated that UTDR with a sound intensity calculation is a powerful tool for the non-invasive monitoring of $CaSO_4$ fouling.

This study builds on prior studies using UTDR with sound intensity calculation to study calcium sulfate scaling under different solution concentrations in a spiral-wound RO membrane module. The initial induction time in the change of sound intensity was first used to distinguish between the concentration polarization and scaling deposition phenomenon, so as to provide valuable insights into membrane cleaning and fouling control strat-

egies. Three focused transducers with the frequency of 2.25 MHz were employed and located equidistantly along the feed flow direction in this study. The independent methods, such as the membrane performance, gravimetric and scanning electron microscopy (SEM) analyses were used to corroborate the ultrasonic results.

2. MATERIALS AND METHODS

2.1 Experimental design and UTDR measurement systems

Fig. 1 is a schematic diagram of the RO desalination and UTDR measurement system. The assembly consisted of three 100 L feed tanks for storage and supply of the scaling solution and pure water, a cooling system for the feed tanks, a feed pump and a high-pressure pump for the pressurization of the feed solution, analog pressure gages and valves, and a by-pass line parallel to the test module. The by-pass line was used to adjust both the flow rate and the pressure inside the cell. The pressure was controlled by means of a back pressure regulator on the outlet line of the element. The permeate and retentate streams were circulated back to the feed tank in the experimental set-up. Two conductivity meters (C1 and C2) were installed to measure the concentration of the feed and permeate. Brine and permeate flow from the module were measured by a flow meter and manually controlled by the valves (V1~V3). The CSM RE4021-TL SWRO elements with a membrane area of 3.30 m^2 and a stainless steel module housing with 105.5 mm outside diameter and 2.0 mm thickness were used during the experiments. The RO membrane (RE4021-TL, CSM) is a polyamide thin-film composite membrane. The maximum operating pressure and water recovery were 2.5 MPa and 75%, respectively.

As also shown in Fig. 1, the ultrasonic measurement system consisted of three 2.25 MHz ultrasonic transducers, a pulser-receiver (Panametrics 5058PR), and a 350 MHz digital oscilloscope (Agilent 54641A). The oscilloscope connected to the pulser-receiver captured and displayed the data signal as amplitude changes on its front panel. Each set of ultrasonic data generated consisted of 2000 data points. This data can be stored on a computer's hard drive. The ultrasonic data can be further analyzed by MS Excel. Three transducers (TD1, TD2 and TD3) were mounted on the outside of the module housing with 452 mm length along the feed flow direction. TD2 was fixed in the middle of the module. The distance between TD1 and TD2, and TD2 and TD3 were 150 mm. Castor oil was used as a couplant to couple the transducer.

2.2 Ultrasonic signal analysis and the sound intensity calculation

The sound intensity calculation and modeling were based upon the original ultrasonic spectrum measured at different operation times (An et al., 2011). For example, while the spectrum is obtained, the sound pressure can be calculated by Eq.(1):

$$P_i(t) = A_i \sin[\frac{2\pi}{T_a}(t - t_0)] \quad (1)$$

where T_a is the average period of each subsection (s), A_i is the amplitude of peaks (V), t is the instantaneous phase angle, and t_0 is the initial phase angle determined by the arrival time of peaks.

The sound pressure of the spectrum was then obtained by using Mathematical software (Wolfram Research Inc.). The sound intensity I is determined by Eq.(2):

$$I = \frac{\int_0^T P^2 dt}{T\rho_0 C_0} \quad (2)$$

where ρ_0 is the medium density (kg/m^3), T is the corresponding arrival time in the spectrum (s) and C_0 is the ultrasound velocity in the medium (m/s).

Therefore, the acoustic spectra obtained during the membrane fouling were expressed by sound intensity, which is related to the sound pressure, the medium density and sound velocity etc. The sound intensity (W/m^2) was calculated and plotted by the Mathematical software. The relative sound intensities as a function of operation time were determined on the basis of the percentage of the sound intensity of the reference spectrum. The spectrum obtained at the initial fouling operation time was referred to as the reference spectrum. Finally, the relationship between changes in the acoustic response signals and its total sound intensity and the formation of the scaling during the fouling/cleaning experiments would be obtained.

2.3 Experimental procedure

The scaling experiments were carried out with 1.0 g/L and 2.0 g/L calcium sulfate solution. The key characteristics of the feed solutions (1 g/L and 2 g/L $CaSO_4$) were summarized in Table 1. The saturated concentration of $CaSO_4$ is 2.5 g/L at the temperature of 25°C. Each experiment consisted of two phases. First, the membrane elements was placed inside the cell with pure water being circulated through the system at the desired flow rate and an applied pressure of 1.0±0.1 MPa for 3 h to achieve steady states of membrane module performance and UTDR signals. The pure water flux remained essentially constant at 50.0 L/m^2·h MPa during the water equilibration phase. The state of the module in the pure water phase was treated as the reference. All the experiments were carried out at the same operation pressure of 1.0±0.1 MPa with a flow rate of 60.0 ±1.0 L/h while the temperature was controlled at 25.0 ±1.0°C. Once a steady state with respect to the permeate flux and the ultrasonic spectra were attained, the feed was switched to the feed solution to initiate the scaling phase, in which the permeate flux and ultrasonic reflection signals of RO elements were measured at regular intervals. The experiments were continued until the ultrasonic responses and permeate flux was stabilized.

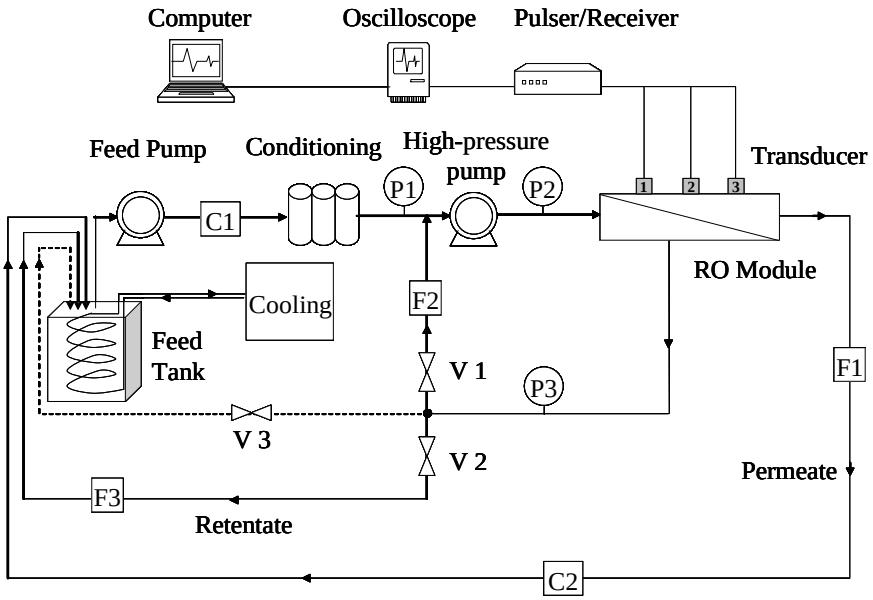

Figure 1 Schematic diagram of the RO desalination and UTDR measurement system

Table 1 Key characteristics of feed solutions

Constituent	Feed solution with 1 g/L $CaSO_4$	Feed solution with 2 g/L $CaSO_4$
pH	6.8	7.2
Conductivity (μs/cm)	1526	2000
Total hardness (mg/L as $CaCO_3$)	750	1480

After the scaling experiment, the cleaning process was conducted. Water flushing was used to clean the fouled SWRO module. Before the cleaning experiment, the feed solution was changed to pure water at the same operation condition of the scaling experiment, so that the pure water flux and the UTDR signals could be obtained in real time. The cleaning phase was conducted until the ultrasonic response and permeate flux was stabilized.

In addition, membrane autopsy studies were carried out with the fouled membranes after 90 h of the scaling experiment. The membrane module was drained and removed from the housing. After allowing it to dry at room temperature for approximately two weeks, the element was opened mechanically and the fouled or cleaned envelope layers were counted and marked from outmost to innermost (closest to the pure water tube) with 1st to 27th before the module was unrolled (An et al., 2011). Then the marked envelope layers were carefully cut into the narrow rectangle sample with a 20.0 mm width along the feed flow direction. The fouled membrane samples were collected from seven different sections marked by A through G along the feed flow direction (at a gap of 55.0 mm wide) of the fouled element and subsequently stored. In order to provide a quantitative analysis for the fouling deposition in the spiral-wound module, the gravimetric measurements were conducted by comparing the mass of test membrane sample from A to G to that of clean membrane sample used as a reference. The coverage of $CaSO_4$ scaling has been obtained by comparing the deposit mass with the relative membrane area.

Furthermore, in order to reveal different morphologies on the subsections from A to G along the feed flow direction, the membrane samples were taken out for the morphological analysis by SEM (QUANTA200, FEI) after the gravimetric measurements.

3. RESULTS AND DISCUSSIONS

3.1 Effect of $CaSO_4$ solution concentration on filtration performance

As shown in Fig. 2a, the normalized flux at feed solution of 1 g/L $CaSO_4$ gradually decreased to 63% of its initial value after 90 h of fouling operation. However, the normalized flux obtained at feed solution of 2 g/L $CaSO_4$ rapidly decreased to 41.2% of its initial value after 10 h of fouling operation, and then gradually dropped to 19.7% of its initial value at the end of the fouling experiment. The rapid drop of flux is due to the concentration polarization (Tun et al., 2005). Afterwards the gradual decline is attributed to the formation and growth of the scaling layer on the membrane surface (Tang et al., 2010). It also can be seen in Fig. 2a that the normalized flux decline during the fouling operation with 2 g/L $CaSO_4$ was more significant than that with 1g/L $CaSO_4$. It indicated that the whole membrane module suffered from more severe fouling at the higher feed solution of 2 g/L $CaSO_4$.

It can be seen from Fig. 2b that the conductivity at feed solution of 2 g/L $CaSO_4$

rapidly decreased from 2000 μs/cm to 1286 μs/cm at the initial 10 h of fouling operation and then gradually decreased to 1122 μs/cm after 90 h of fouling operation. However, the conductivity at feed solution of 1 g/L $CaSO_4$ gradually decreased from 1526 μs/cm to 1174 μs/cm during 90 h of fouling operation. Based on the mass balance, the decrease in the conductivity of feed solution was ascribed to the $CaSO_4$ precipitation on the membrane surface as the fouling progressed. The amount of $CaSO_4$ precipitation on the membrane surface were 22.9 g and 87.8 g after 90 h of fouling operation carried out with the 1 g/L and 2 g/L $CaSO_4$, respectively. Moreover, the rejection of the membrane at both feed solution concentration had a slight drop and maintained above 98% through the scaling process (Fig. 2c). It implied that the high feed concentration caused more inorganic salts to deposit on membranes surface. These observations revealed that the whole membrane module at the high feed solution of 2 g/L $CaSO_4$ suffered from more severe fouling.

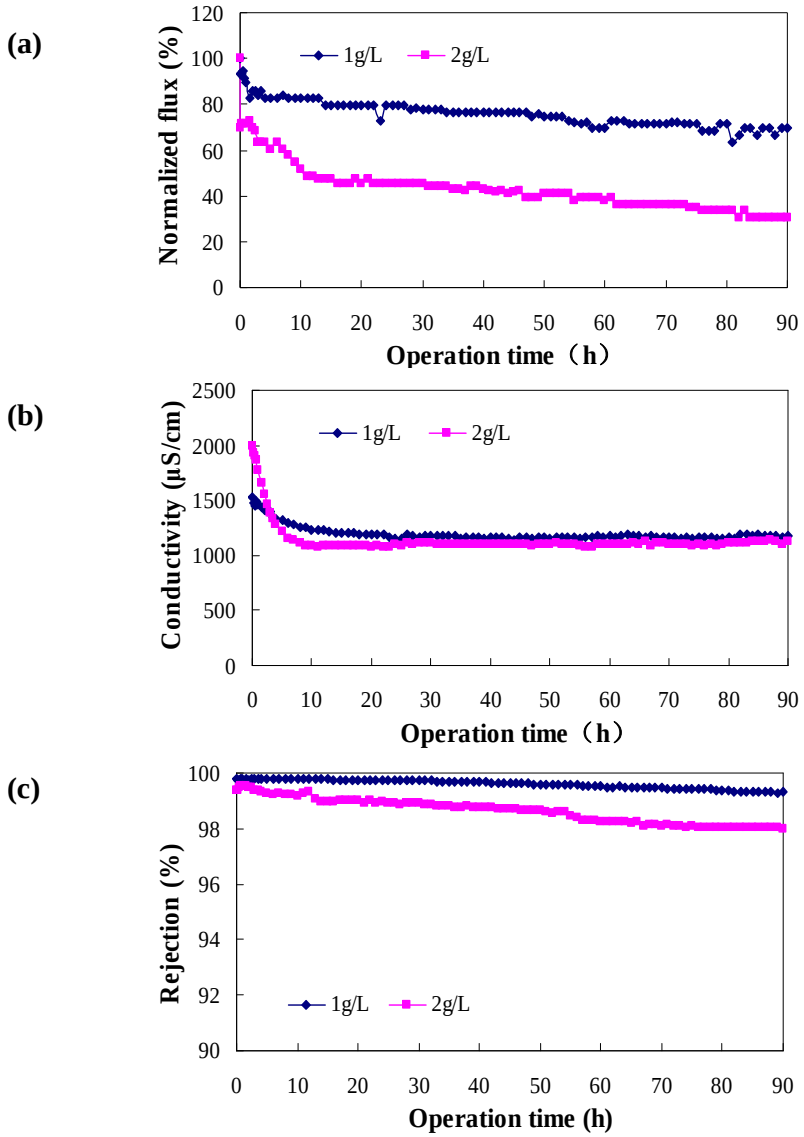

Figure 2 The normalized flux (a), feed conductivity (b) and rejection (c) vs. operation time during the fouling experiments carried out with 1 g/L and 2 g/L $CaSO_4$

3.2 Ultrasonic measurements based on sound intensity calculation

The ultrasonic spectra obtained by three ultrasonic transducers TD1-TD3 during fouling experiments were shown in Figs. 3-5, respectively. It can be seen in Figs. 3-5 that by comparison to the ultrasonic spectra obtained by TD1 and TD2, the great changes in the ultrasonic spectra obtained by TD3 were observed in the range of arrival time from 20 to 50 μs during fouling experiments. The change of the ultrasonic spectra is ascribed to the formation of the fouling layer on the membrane surface (Sanderson et al., 2002). It indicated that the fouling degree gradually increased along the flow direction of RO module. It also can be seen in Figs. 3b-5b that the ultrasonic signal spectra in amplitude-domain decayed at a range of the arrival time from 20 μs to 50 μs at initial 60 h of fouling operation carried out with 2 g/L $CaSO_4$, whereas partly resumed in the following operation (90 h). However, the ultrasonic signal spectra in amplitude-domain gradually decreased during the whole 90 h of fouling operation with 1 g/L $CaSO_4$ (Figs. 3a-5a).

Although individual peaks represent a complex superposed reflection from the close-packed interfaces relative to the nature of fouling processes, it is hard to reveal the relationship between ultrasonic signal responses and fouling deposition only from the UTDR observations. Thus, UTDR based on sound intensity calculation and modeling was developed to investigate the fouling processes with operation time.

It can be seen in Fig. 6 that the relative sound intensity obtained with TD1, TD2 and TD3 kept stable at the initial fouling phase, and then began to decrease after 25 h, 15 h and 5 h of fouling experiment carried out with 2 g/L $CaSO_4$, respectively. Similarly, the duration of stable relative sound intensity was 30 h, 25 h and 10 h for the TD1, TD2 and TD3 during filtration of 1 g/L $CaSO_4$, respectively. It indicated that there exist different induction times in the changes of the relative sound intensity along the feed flow direction at the initial lag phase. And at the same position of RO module, the induction time obtained in the fouling experiment with 1 g/L $CaSO_4$ is obviously longer than that with 2 g/L $CaSO_4$, which is ascribed to the difference of salt saturation level on the membrane surface under different feed solution concentrations (Gloede and Melin, 2008; Hasson et al., 2001).

It also can be seen in Fig. 6 that the relative sound intensity obtained with 2 g/L $CaSO_4$ kept stable at the initial fouling phase, then declined to the minimum and resumed in the following operation. For example, the relative sound intensity obtained with TD2 kept stable in the first 5 h of fouling operation. Then it took 55 h of fouling time gradually to reach the relative minimum sound intensity of 39.8%. Afterwards, the relative sound intensity increased to 68.9% after 90 h of fouling time. The reason was that the growing precipitate under the transducer interfered with the echo signal from the module by absorption and scattering, thus leading to the decrease of sound intensity. Once a fouling layer formed, an intensive reflected wave occurred from the water/fouling interface due to the calcium-sulfate density of 2.61 g/cm^3 which ultrasonic impedance is higher than that of polymeric membrane materials (Chai et al., 2007). Thus the sound intensity would partly resume with the formation of a reasonably thick and uniform fouling. However, unlike the profile of relative sound intensity obtained with 2 g/L $CaSO_4$, the relative sound intensity obtained with 1 g/L $CaSO_4$ kept stable at initial fouling phase, and then gradually decreased to stable value (Fig. 6). It may be ascribed to the different structures of fouling layer (Bao et al., 2010).

In summary, these ultrasonic measurements revealed that the higher concentration of feed

solution is, the shorter the induction time is and the more severe the membrane fouling gets.

3.3 Gravimetric measurements and SEM analysis

In order to confirm the above ultrasonic measurements, the fouled membranes after 90 h of fouling operation were taken for the SEM and gravimetric analysis. The SEM micrographs of the fouled membrane samples along flow direction with different feed solution concentrations are shown in Fig. 7. Obviously, the fouling coverage increased gradually along the flow direction. It can be observed in Fig. 7a that a few microcrystal strands covered on the fouled membrane surface from D to G obtained at the low feed solution concentration of 1 g/L $CaSO_4$ (Fig. 7a), whereas plenty of both acicular and clusters crystals formed on the membrane surface from D to G obtained at the high feed solution concentration of 2 g/L $CaSO_4$ (Fig. 7b), leading to the rough scaling layer. It would result in scattering of ultrasonic signal. This is the reason why the relative sound intensity declined to the minimum and resumed at feed solution concentration of 2 g/L $CaSO_4$ as shown in Fig. 6.

In order to further provide a quantitative analysis for the fouling deposition, the scaling coverage obtained by gravimetric measurements is presented in Fig. 8. The scaling coverage along the flow direction increased from 2.6 g/m^2 at specimen A to 20.3 g/m^2 at specimen G during filtration of 1 g/L $CaSO_4$. Similarly, the scaling coverage with 2 g/L $CaSO_4$ increased from 2.6 g/m^2 at specimen A to 42.4 g/m^2 at specimen G. It is quite likely that a high concentration polarization leads to the greater scaling coverage at the downstream (Shi et al., 2005). It also can be seen in Fig. 7 that at the same position of the sample, the coverage obtained with the feed solution of 2 g/L $CaSO_4$ is higher than that obtained with the feed solution of 1 g/L $CaSO_4$. In summary, the gravimetric and the SEM analysis are in well agreement with the UTDR measurements.

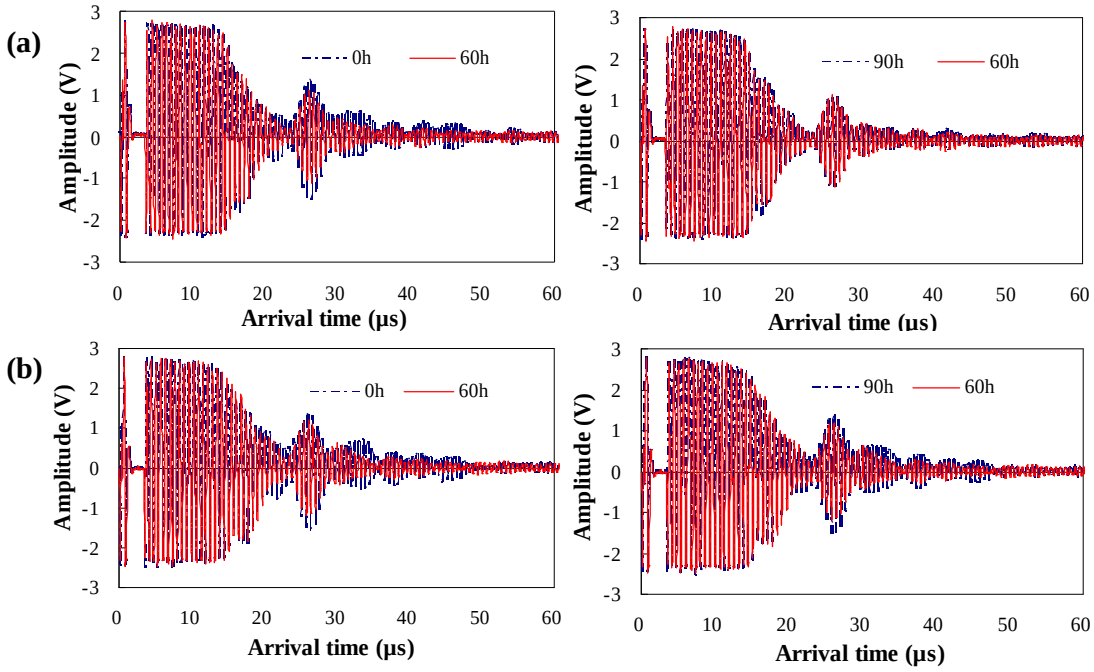

Figure 3 Ultrasonic response signals obtained by TD1 at different operation times of fouling experiments (Feed solution: (a) 1 g/L and (b) 2 g/L $CaSO_4$)

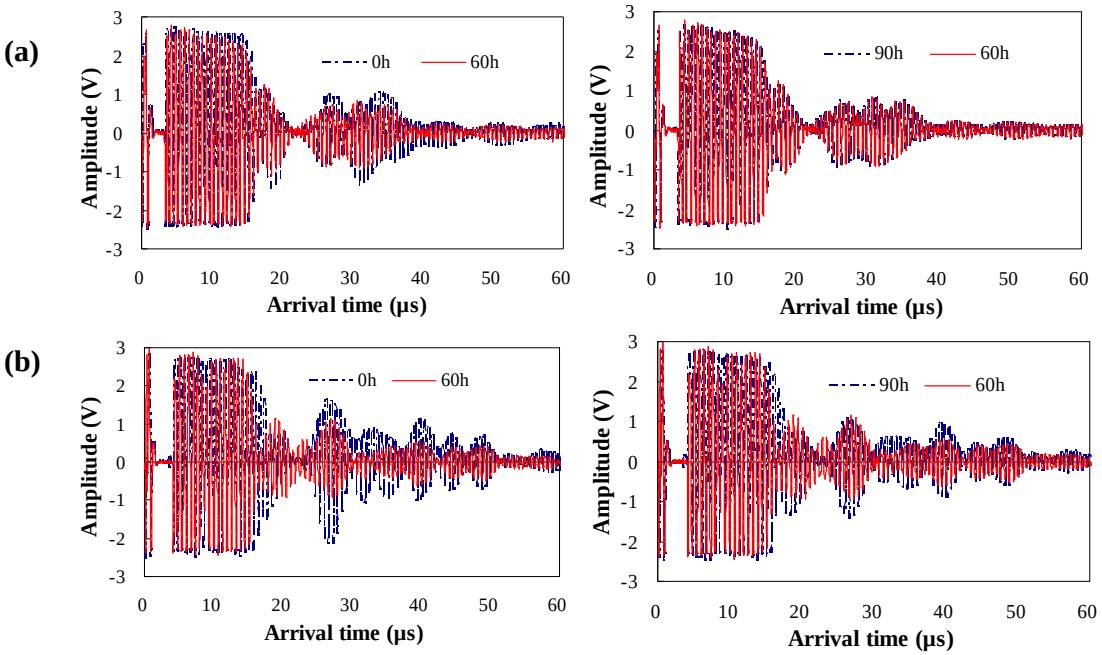

Figure 4 Ultrasonic response signals obtained by TD2 at different operation times of fouling experiments (Feed solution: (a) 1 g/L and (b) 2 g/L $CaSO_4$)

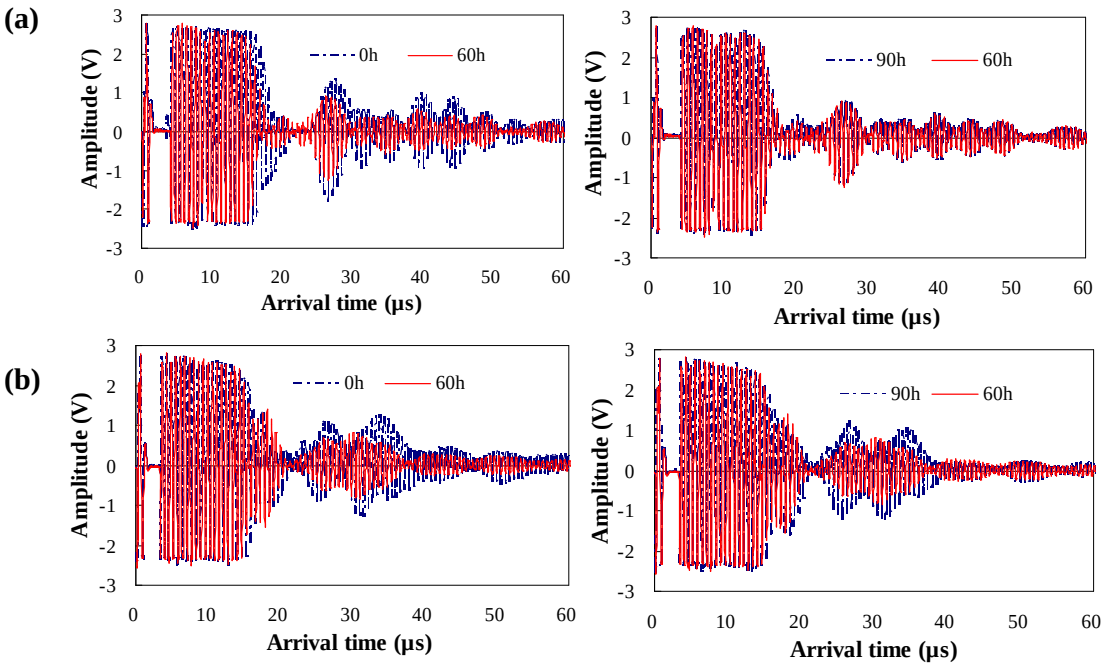

Figure 5 Ultrasonic response signals obtained by TD3 at different operation times of fouling experiments (Feed solution: (a) 1 g/L and (b) 2 g/L $CaSO_4$)

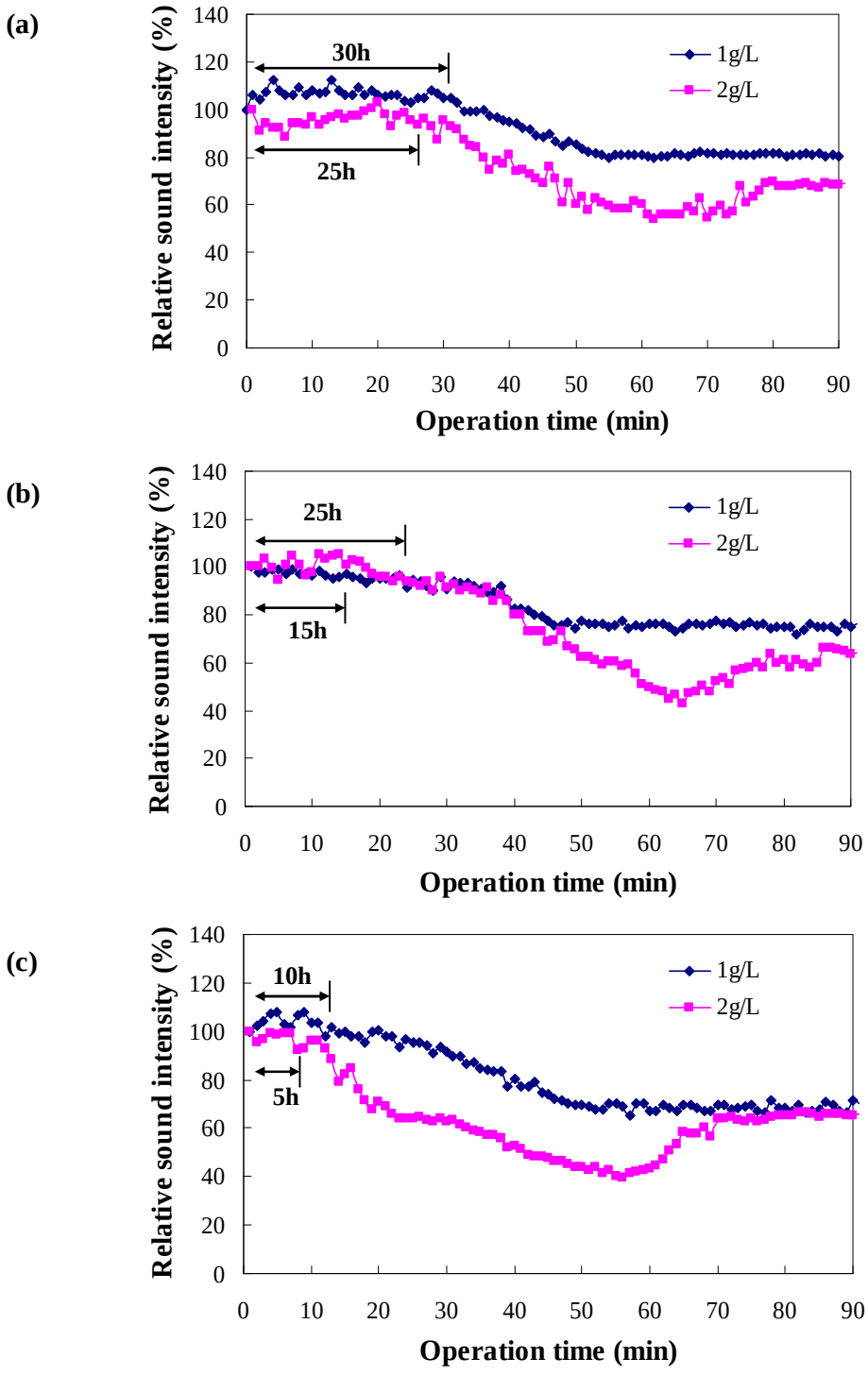

Figure 6 The relative sound intensity obtained by (a) TD1, (b) TD2 and (b) TD3 vs. operation time during fouling experiments carried out with 1 g/L and 2 g/L $CaSO_4$

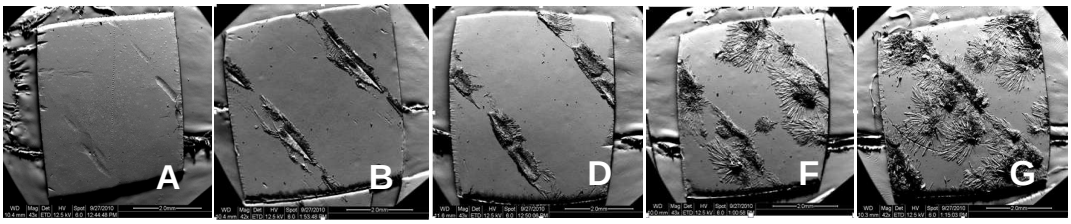

(a)

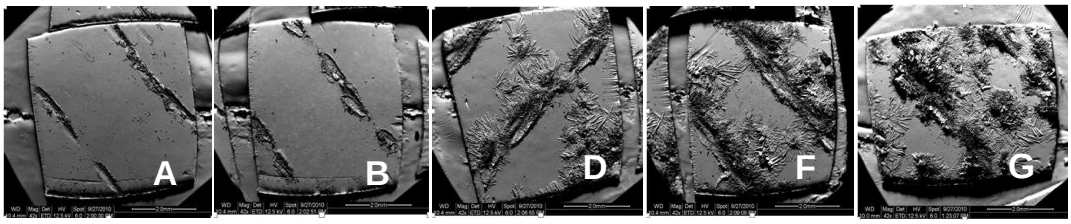

(b)

Figure 7 SEM micrographs of fouled membrane samples obtained from the 9th membrane envelope layer along the fluid direction of the spiral-wound RO module after 90 h of fouling experiment (Feed solution: (a) 1 g/L and (b) 2 g/L $CaSO_4$)

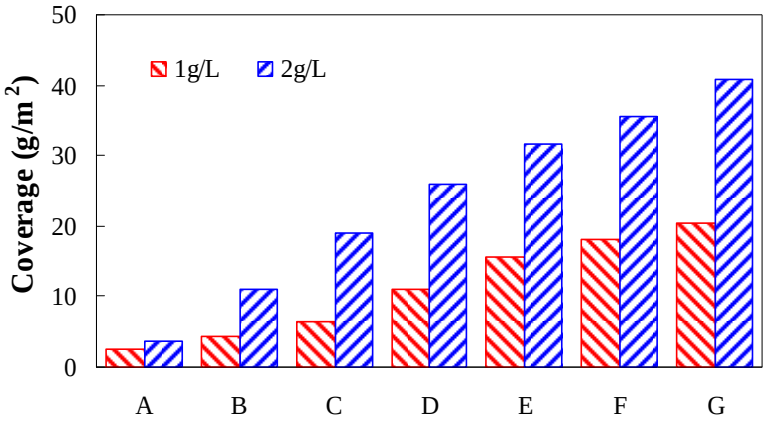

Figure 8 Gravimetric analysis of the membrane samples obtained after 90 h of fouling operation carried out with 1 g/L and 2 g/L $CaSO_4$

Table 2 Relative sound intensity obtained by TD1-TD3 before and after water flush at different operation times of fouling experiment carried out with 1 g/L $CaSO_4$

	Relative sound intensity (%)					
	TD1		TD2		TD3	
	30h	35h	25h	30h	10h	13h
Before water flush	95.0±0.5	90.0±0.8	93.5±0.6	93.0±0.5	98.0±0.4	96.0±0.7
After water flush	99.5±0.3	93.0±0.5	99.6±0.3	94.5±0.8	99.8±0.2	97.5±0.6

Table 3 Relative sound intensity obtained by TD1-TD3 before and after water flush at different operation times of fouling experiment carried out with 2 g/L $CaSO_4$

	Relative sound intensity (%)					
	TD1		TD2		TD3	
	25h	30h	15h	18h	5h	8h
Before water flush	90.0±1.0	85.0±1.0	97.0±0.8	93.0±0.8	97.5±0.6	90.0±1.0
After water flush	99.6±0.3	90.0±0.6	99.8±0.2	95.0±0.8	99.8±0.2	92.5±1.0

3.4 Concentration polarization phenomenon

In order to further investigate the concentration polarization phenomenon, water flushing was used to clean the fouled RO module after a certain time symbolized by T of fouling operation. If the ultrasonic signal response after water flushing was resumed to the ultrasonic responses at the start of fouling operation, the certain time T was regarded as demarcation point between the concentration polarization and scaling deposition phenomenon. Namely, before the certain time T, the membrane fouling was mainly caused by concentration polarization. After the certain time T, the membrane fouling was mainly caused by formation and growth of scaling layer. This is ascribed to the clear distinction between the concentration polarization and the scaling deposited on membrane surface. In irreversible fouling, the inorganic scaling will appear at the solute-membrane interaction. However, the concentration polarization leads to gel formation, whereas reversible fouling could be removed by wash flush (Matthiasson and Sivik, 1980).

It can be seen in Table 2 that after 30 h of fouling operation carried out at 1 g/L $CaSO_4$, the relative sound intensity obtained by TD1 decreased to 95%. After the water flush, the relative sound intensity obtained by TD1 increased to 99.5%. However, after 35 h of fouling operation, the relative sound intensity obtained by TD1 decreased to 90%, whereas the relative sound intensity could only increase to 93% after water flush. It indicated that 35 h of fouling time was regarded as the duration of concentration polarization. Similarly, the duration of concentration polarization at the position detected by TD2 and TD3 was 30 h and 13 h, respectively (Table 2). An interesting phenomenon was observed that the duration of concentration polarization at the position detected by TD1-TD3 (35 h, 30 h and 13 h in Table 2) lag behind the induction time (30 h, 25 h and 10 h in Fig. 6). These observations indicated that the induction time could be an indicator for the start of foulants deposition.

A similar trend also can be seen during the fouling operation at 2 g/L $CaSO_4$ as shown in Table 3. The duration of concentration polarization at the position detected by TD1-TD3 was 30 h, 18 h and 8 h, which is longer than the induction time obtained with TD1-TD3 (25 h, 15 h and 5 h) in Fig. 6, respectively. Overall, the UTDR based on sound intensity calculation and modeling could effectively predict the duration of concentration polarization. It could provide some basis for the control of membrane fouling in RO.

CONCLUSIONS

UTDR technique with the sound intensity calculation was extensively used to detect $CaSO_4$ fouling and concentration polarization in spiral-wound RO membrane module under

different solution concentrations. The sound intensity gradually decreased to the stable value during filtration of 1.0 g/L $CaSO_4$ due to the deposition of the foulants on the membrane surface. However, the sound intensity obtained in the fouling experiment carried out with the solution of 2 g/L $CaSO_4$ gradually decreased to minimum at first, and then increased, which is ascribed to the scaling deposition and the formation of fouling layer on the membrane surface. Furthermore, the duration of concentration polarization and the beginning of $CaSO_4$ scaling could be monitored by the change of sound intensity. The ultrasonic results have a good agreement with the independent measurements including gravimetric measurements and SEM analysis. Overall, the ultrasonic technique provides new insight into the prevention and control of membrane fouling in spiral-wound RO modules.

ACKNOWLEDGMENTS

This work was financially supported by the Commonweal Project of China National Ocean Bureau (No. 201105025) and Chang-jiang Scholars and Innovative Research Team in University of Ministry of Education of China (Grant No. IRT13084).

REFERENCES

An, G.H., Lin, J.B., Li, J.X. and Jian, X.Q. (2011). In situ monitoring of membrane fouling in spiral-wound RO modules by UTDR with a sound intensity modeling. *Desalination and water Treatment*, 32(1-3), 226-233.

An, G.H., Lin, J.B., Li, J.X., Li, X.H. and Jian, X.Q. (2011). Non-invasive measurement of membrane scaling and cleaning in spiral-wound reverse osmosis modules by ultrasonic time-domain reflectometry with sound intensity calculation. *Desalination*, 283, 3-9.

Bao, S.X., Zhang, Y.M., Liu, T., Huang, J. and Chen, T.J. (2010). Evolution and morphometric characterization of fouling on membranes during the desalination of high $CaSO_4$ supersaturated water by electrodialysis. *Desalination*, 256(1-3), 94-100.

Chai, G.Y., Greenberg, A.R. and Krantz, W.B. (2007). Ultrasound, gravimetric, and SEM studies of inorganic fouling in spiral-wound membrane modules. *Desalination*, 208(1-3), 277-293.

Chong, T.H., Wong, F.S. and Fane, A.G. (2007). Enhanced concentration polarization by unstirred fouling layers in reverse osmosis: Detection by sodium chloride tracer response technique. *Journal of Membrane Science*, 287(2), 198-210.

Chong, T.H., Wong, F.S. and Fane, A.G. (2008). The effect of imposed flux on biofouling in reverse osmosis: Role of concentration polarisation and biofilm enhanced osmotic pressure phenomena. *Journal of Membrane Science*, 325(2), 840-850.

Gloede, M. and Melin, T. (2008). Physical aspects of membrane scaling. *Desalination*, 224(1-3), 71-75.

Hasson, D., Drak, A. and Semiat, R. (2001). Inception of CaSO4 scaling on RO membranes at various water recovery levels. *Desalination*, 139(1-3), 73-81.

Li, J., Sanderson, R.D., Chai, G.Y. and Hallbauer, D.K. (2005). Development of an ultrasonic technique for in situ investigating the properties of deposited protein during crossflow ultrafiltration. *Journal of Colloid and Interface Science*, 284(1), 228-238.

Mairal, A.P., Greenberg, A.R., Krantz, W.B. and Bond, L.J. (1999). Real-time measurement of inorganic fouling of RO desalination membranes using ultrasonic time-domain reflectometry. *Journal of Membrane Science*, 159(1-2), 185-196.

Mairal, A.P., Greenberg, A.R. and Krantz, W.B. (2000). Investigation of membrane fouling and cleaning using ultrasonic time-domain reflectometry. *Desalination*, 130(1), 45-60.

Matthiasson, E. and Sivik, B. (1980). Concentration polarization and fouling. *Desalination*, 35, 59-103.

Mulder, M. (1991). *Basic Principles of Membrane Technology*. Kluwer Academic Publishers, Dordrecht, Netherland.

Song, L.F. and Liu, C. (2012). A total salt balance model for concentration polarization in cross-flow reverse osmosis channels with shear flow. *Journal of Membrane Science*, 40(1-2), 313-322.

Sanderson, R.D., Li, J.X., Koen, L.J. and Lorenzen, L. (2002). Ultrasonic time-domain reflectometry as an on-destructive visualization technique to monitor fouling and cleaning on reverse osmosis membranes. *Journal of Membrane Science*, 20(7), 105-117.

Shi, W.Y., Rahardianto, A., Lee, R.W. and Cohen, Y. (2005). Morphometric characterization of calcium sulfate dihydrate (gypsum) scale on reverse osmosis membranes. *Journal of Membrane Science*, 252(1-2), 253-263.

Tun, C.M., Fane, A.G., Matheickal, J.T. and Sheikholeslami, R. (2005). Membrane distillation crystallization of concentrated salts-flux and crystal formation. *Journal of Membrane Science*, 257(1-2), 144-155.

Tang, C.Y., She, Q, WinsonLay, C.L., Wang, R. and Fane, A.G. (2010). Coupled effects of internal concentration polarization and fouling on flux behavior of forward osmosis membranes during humic acid filtration. *Journal of Membrane Science*, 354(1-2), 123-133.

Zhang, Z.X., Bright, V.M. and Greenberg, A.R. (2007). Use of capacitive microsensors and ultrasonic time-domain reflectometry for in-situ quantification of concentration polarization and membrane fouling in pressure-driven membrane filtration. *Sensors and Actuators B: Chemical*, 117(2), 323-331.